

Mapping residual stereopsis in macular degeneration

Preeti Verghese

Smith-Kettlewell Eye Research Institute, San Francisco,
CA, USA



Saeideh Ghahghaei

Smith-Kettlewell Eye Research Institute, San Francisco,
CA, USA



Zachary Lively

Smith-Kettlewell Eye Research Institute, San Francisco,
CA, USA



Individuals with macular degeneration typically lose vision in the central region of one or both eyes. A binocular scotoma occurs when vision loss occurs in overlapping locations in both eyes, but stereopsis is impacted even in the non-overlapping region wherever the visual field in either eye is affected. We used a novel stereoperimetry protocol to measure local stereopsis across the visual field (up to 25° eccentricity) to determine how locations with functional stereopsis relate to the scotomata in the two eyes. Participants included those with monocular or binocular scotomata and age-matched controls with healthy vision. Targets (with or without depth information) were presented on a random dot background. Depth targets had true binocular disparity of 20' (crossed), whereas non-depth targets were defined by monocular cues such as contrast and dot density. Participants reported target location and whether it was in depth or flat. Local depth sensitivity (d') estimates were then combined to generate a stereopsis map. This stereopsis map was compared to the union of the monocular microperimetry estimates that mapped out the functional extent of the scotoma in each eye. The “union” prediction aligned with residual stereopsis, showing impaired stereopsis within this region and residual stereopsis outside this region. Importantly, the stereoblind region was typically more extensive than the binocular scotoma defined by the intersection (overlap) of the scotomata. This explains why individuals may have intact binocular visual fields but be severely compromised in tasks of daily living that benefit from stereopsis, such as eye–hand coordination and navigation.

Introduction

This study investigates residual stereopsis in macular degeneration (MD), which is a highly prevalent, usually age-related disease that affects the central retina, including the fovea. It affects 13.4% of the U.S.

population over age 60 (Klein, Chou, Klein, Zhang, Meuer, & Saaddine, 2011) and occurs in two forms: dry and wet (e.g., Hubschman, Reddy, & Schwartz, 2009). Both types of MD can lead to bilateral scotomata (Schuchard, Naseer, & de Castro, 1999; Cheung & Legge, 2005) where the spatial extent of the visual field defect depends on how much the scotomata in the two eyes overlap. When the overlapping scotoma locations in the two eyes include the fovea, the resultant binocular central field loss (CFL) can significantly impact daily life, particularly tasks that require high-acuity vision, such as reading, recognizing faces, and finding items of interest (Legge, Ross, Isenberg, & LaMay, 1992; Fine & Peli, 1995; Fletcher, Schuchard, & Watson, 1999; Chung, 2011). Binocular CFL also leads to the adoption of a peripheral retinal locus (PRL) for fixation, which presents challenges for voluntary eye movements (White & Bedell, 1990).

It is less appreciated that, even when the scotomata in the two eyes do not overlap significantly, individuals experience loss of stereopsis in the parts of the visual field that have scotomata in either eye. Although individuals become acutely aware of their vision loss when they have a binocular scotoma, non-overlapping scotomata can lead to less obvious, but serious consequences. In cases where there is little or minimal overlap between the scotomata in the two eyes, the acuity loss may be small, but stereopsis may be impacted in the part of the visual field that has vision loss in *either* eye. In the special case when there is a significant central scotoma in only one eye, binocular acuity may be preserved while stereopsis is severely impacted. Thus, the loss of stereopsis has the potential to impact eye–hand coordination (Melmoth, Finlay, Morgan, & Grant, 2009; Cao & Markowitz, 2014; Verghese, Tyson, Ghahghaei, & Fletcher, 2016; Niechwiej-Szwedo, Colpa, & Wong, 2019) and mobility (Hayhoe, Gillam, Chajka, & Vecellio, 2009; Buckley, Panesar, MacLellan, Pacey, & Barrett, 2010; Bonnen,

Citation: Verghese, P., Ghahghaei, S., & Lively, Z. (2022). Mapping residual stereopsis in macular degeneration. *Journal of Vision*, 22(13):7, 1–13, <https://doi.org/10.1167/jov.22.13.7>.



Matthis, Gibaldi, Banks, Levi, & Hayhoe, 2019), under binocular, real-world viewing conditions.

Individuals with MD typically have asymmetric scotomata in the two eyes and thus rarely have preferred retinal loci at corresponding locations, compromising their ability to see depth from disparity at or near their dominant eye PRL (Verghese & Ghahghaei, 2020). They perform poorly on clinical tests of stereopsis such as the Randot Stereo Test because they fixate the small stereo target with their better-eye PRL, which may not correspond to an intact retinal location in the other eye. As macular degeneration affects the central retina, we expect fine stereopsis to be particularly impaired. Nevertheless, peripheral vision is usually preserved and can support coarse stereopsis, which is helpful for tasks of daily living (Cao & Markowitz, 2014; Verghese et al., 2016). Awareness of which parts of the visual field support stereopsis in CFL can help with individualized rehabilitation techniques to improve eye–hand coordination or navigation. The novel contribution of this study is the measurement of stereopsis in local regions across the visual field to determine whether the region of stereo loss corresponds to the union of the two eyes' scotomata and, more importantly, to examine the potential of the relatively intact periphery to mediate coarse stereopsis. Our stereoperimetry method, which is analogous to the perimetry techniques used to determine visual field loss but with local stereoscopic stimuli (Verghese & Ghahghaei, 2018), demonstrates two findings: First, the intact periphery does indeed mediate coarse stereopsis, and, second, the union of the scotomata in the two eyes can predict the region of stereo loss in the central visual field.

Methods

Participants

Eleven adults with macular degeneration (57–87 years old; seven females) and four age-matched controls (61–74 years old; three females) participated in this study. Seven participants with MD had central field loss due to scotomata in both eyes (referred to as the binocular scotoma group, which included five with age-related MD, one with Best's disease, and one with Stargardt's disease). Four participants with MD had no central field loss because they had either monocular scotomata or non-overlapping scotomata in the two eyes (collectively referred to as the monocular scotoma group, which included three with MD and one with a macular hole). The control participants had normal vision or vision that could be corrected to normal. As the participants with binocular MD chose not to wear their spectacle corrections, we had all observers (monocular MD and controls) not wear their spectacles for the stimulus presented at a viewing distance of 40 cm. Visual acuity without correction is reported for all participants in Table 1. Most participants with scotoma (with the exception of M4 and B7) were referred to us by the low-vision rehabilitation practice of Donald C. Fletcher, MD, at the Pacific Vision Foundation (San Francisco, CA). All experimental procedures were approved by the Institutional Review Board of the Smith-Kettlewell Eye Research Institute and followed the tenets of the Declaration of Helsinki. All participants gave informed written consent after an explanation of the nature of the study and received

ID	Sex	Age	DE acuity (logMAR)	DE PRL (°)	NDE acuity (logMAR)	NDE PRL (°)	Stereoacuity (arcmins)	Diagnosis
Patients								
B1	F	87	0.52	4.74	1.18	7.28	>30	CNV
B2	F	77	0.7	5.5	0.7	7.5	19.6	B
B3	F	77	0.4	1.06	0.81	1.07	>30	CNV
B4	F	77	1.1	7.38	1.2	9.05	19.7	GA
B5	M	57	1.1	5.82	1.2	5.1	19.2	S
B6	M	77	1.12	15.86	1.14	17.41	30	GA
B7	F	72	0.18	0.85	0.84	3.14	1.67	GA
M1	M	80	0.0	N/A	0.4	2.29	19.2	CNV
M2	M	75	0.5	N/A	0.6	3.21	>30	MH
M3	F	90	0.0	N/A	0.1	1.80	13.3	CNV
M4	F	79	0.1	1.80	0.42	6.89	>30	CNV + GA
Controls								
C1	F	78	0.28	—	0.44	—	0.67	—
C2	F	77	0.26	—	0.54	—	1.0	—
C3	F	74	0.08	—	0.22	—	1.0	—
C4	F	65	0.44	—	0.62	—	1.67	—

Table 1. Visual acuity without correction for all participants. *Notes:* The causes for the maculopathy were choroidal neovascularization (CNV) or wet macular degeneration, geographic atrophy (GA) or dry macular degeneration, Best's diseases (B), Stargardt's disease (S), or macular hole (MH). DE = dominant eye; NDE = non-dominant eye.

monetary compensation for their participation. Participants' characteristics are summarized in [Table 1](#).

[Table 1](#) lists the gender, age, acuity, and PRL distance of the dominant eye and non-dominant eye, stereoacuity, and cause of maculopathy. The PRL eccentricity was determined by the center of mass of the fixational eye position during a 10-second interval (obtained by fitting a two-dimensional Gaussian to include 95% of the fixational eye positions) and calculating its distance in degrees from the anatomical foveal pit obtained in the optical coherence tomograph (OCT). PRL eccentricity does not apply to the unaffected eye of monocular MD participants and controls who had foveal fixation. The one exception is M4, who had bilateral non-overlapping scotomata as determined by microperimetry but had a dominant eye with a PRL eccentricity of 1.8° (and acuity of 0.1 logMAR), suggesting foveal vision loss. It is possible that she had a relative scotoma in the foveal region of her dominant eye that was not detected because of the high-contrast flashes (0 dB) that we used for microperimetry. Acuity was measured at a distance of 40 cm using MNREAD, and stereoacuity was measured with the Randot Stereo Test. The causes for the maculopathy were choroidal neovascularization or wet macular degeneration, geographic atrophy or dry macular degeneration, Best's diseases, Stargardt's disease, or macular hole.

Stereoperimetry experiment

Apparatus

Shutter glasses (NVIDIA 3D Vision 2; NVIDIA Corporation, Santa Clara, CA) were used to present stereoscopic stimuli, as in previous studies of stereopsis ([Wardle, Bex, Cass, & Alais, 2012](#); [Ghahghaei, McKee, & Verghese, 2019](#)). The glasses were used in conjunction with a 120-Hz ASUS 3D-Ready HDMI monitor (ASUSTek, Taipei, Taiwan) that alternated the view of each eye, updating at 60 Hz per eye. We used Psychtoolbox in MATLAB (MathWorks, Natick, MA) ([Brainard, 1997](#); [Pelli, 1997](#)) to program stimuli for the experiment. We attempted to monitor fixation of the dominant eye with the EyeLink 1000 eye tracker (SR Research, Kanata, ON, Canada) in the tower-mount configuration, which we have successfully used in other eye movement studies with maculopathy participants ([Shandize, Heinen, & Verghese, 2017](#); [Vullings & Verghese, 2021](#)), but the infrared signal used to control the shutters of the stereo glasses for each eye interfered with the infrared signal from the eye tracker in the tower-mount configuration. We then attempted to track fixation with the eye tracker in the table-mount configuration, but the more noisy signal associated with the table-mount configuration at the viewing

distance of 40 cm and the eccentric gaze angle of some of our participants with binocular scotoma made the eye-position signals unreliable. Therefore, participants were asked to fixate the marker, but fixation was not monitored (see [Figure 1](#)).

Experimental procedure

To map the regions of the visual field that were capable of stereopsis, we presented local depth targets at locations across the visual field. The targets were disparity-defined square regions on a full-field random dot background. The random dots were presented at the maximum display luminance of 149 cd/m^2 on a dark background of 1.06 cd/m^2 (Michelson contrast 98.7%). Targets were presented in one of eight directions that included the four cardinal directions and four obliques; a subset of the eccentricities 1° , 2.5° , 5° , 10° , 15° , 20° , and 30° ; and the fovea. Exceptions to these test locations included the following: an extra target location at the dominant-eye PRL and a restriction of test locations to the lower half of the visual field for some participants (C3, M1, M2, B3, B4, B5, and B6). Targets were square regions that subtended 1° at the fovea and were *m*-scaled by eccentricity according to $1 + (\text{target eccentricity}/3)$, according to [Rovamo and Virsu \(1979\)](#). The target was equally likely to be a true depth target or a flat target with a monocular depth cue. Depth stimuli were rendered with a crossed disparity of 20 arcmins (a disparity of 30 arcmins was used for participant B6). Flat stimuli were rendered with one of three monocular cues: (1) the half image associated with one eye (e.g., left) was shown to both eyes, resulting in no disparity between the eyes (this was done separately with the left- and right-eye half images); (2) the left- and right-eye half images were shown to both eyes, resulting in no disparity but an apparent doubling of dot density; or (3) lower contrast for the dots in the target region. The lower contrast dots that were used on "flat trials" had a luminance of 54.5 cd/m^2 or a contrast of 36.6%, compared to the other dots that had a contrast of 98.7%. Each location was tested at least six times, with three disparity targets and three flat targets.

Participants viewed the display binocularly, with their head on a chinrest, and maintained fixation (with their PRL) on a marker whose position from the center of the screen corresponded to the distance of their dominant eye PRL from the fovea. If we tested only the lower visual field of a participant, the vertical position of location corresponding to the fovea was displaced upward to facilitate testing a larger extent of the lower visual field. The random-dot stimulus with the PRL fixation marker was presented on the participant's ready and lasted for 3 seconds. At the end of the trial, participants were asked to report whether

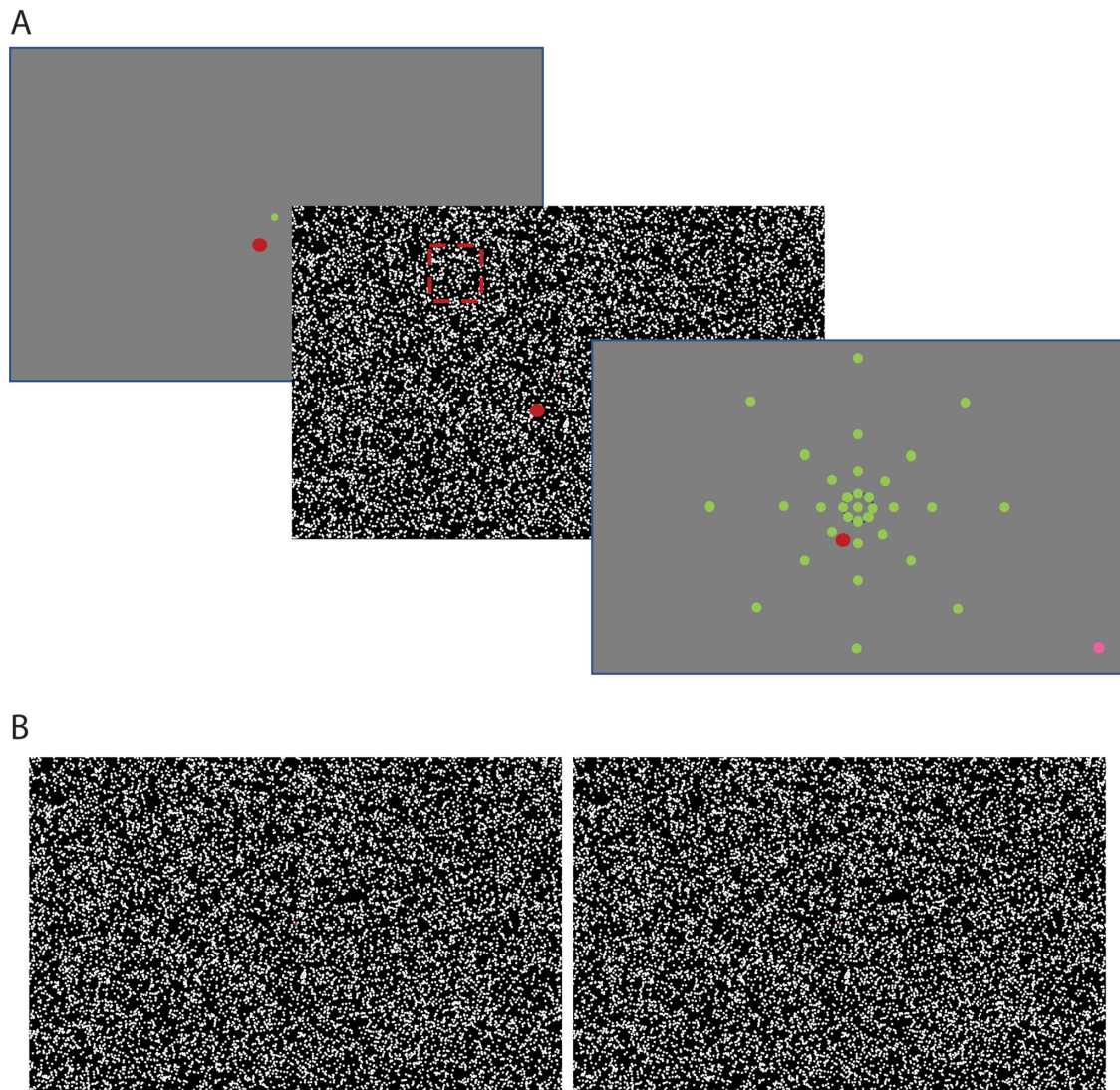


Figure 1. (A) Sequence of a single trial in the stereoperimetry experiment. A trial started with the participant fixating a red fixation marker, placed at the location of the dominant-eye PRL with respect to the fovea location (small green dot) at the center of the screen. The participant then initiated the random-dot stereogram with a key press. The random-dot display had the same fixation marker and either a real depth target or a flat target defined by monocular cues, presented at one of many locations across the screen. A sample target location is shown marked with red dashed lines for purposes of visualization (these lines were not present in the actual display). The random dot display lasted 3 seconds and was followed by a response screen that displayed potential target locations. The participant then responded whether there was a real depth target and selected its location on the response screen. If the participant did not see a square target region, the experimenter clicked the pink dot in the bottom right of the response screen (B). The random dot display intended for cross fusion depicts a square target along the upper left diagonal.

a depth target was present and where it was located. The experimenter recorded the depth present/absent responses using a left/right mouse click at the location that participants selected. If the participant reported “nothing seen,” then a button at the bottom right corner of the screen was clicked so they could advance to the next trial. “Nothing seen” reports were included in our analysis and were counted as misses or correct rejections.

Analysis of stereoperimetry data

Performance in the experiment was quantified by a d' estimate for each stimulus location. The hit proportion for a stimulus location was the number of times participants correctly reported the presence of depth divided by the total number of depth trials at the location. The proportion of false alarms for a stimulus location was the number of times participants

either chose that location for the depth target, when it had occurred at another location, or reported depth at the stimulus location on a no-depth trial. False alarms were summed and divided by the total number of trials minus the number of depth trials at a test location. Proportions of 1 and 0 were adjusted to 0.99 and 0.01, respectively.

Predicting the region of stereo loss from scotoma maps

To estimate the region of stereo loss, we measured the monocular scotomata in each eye using microperimetry. We used an Optos (Optos Inc., Marlborough MA) optical coherence tomograph/scanning laser ophthalmoscope (OCT/SLO) to collect monocular microperimetry data, fixation stability, and foveal pit location, all with a field size of 29.7° . We manually selected the test flash locations in real time to best probe each participant's region of vision loss, or functional scotoma. The absolute scotoma was measured with unattenuated 0-dB flashes with a dot luminance 125 cd/m^2 and a Weber contrast of 12.5. For two participants we also measured the relative scotoma by attenuating the contrast of the flash in 2-dB steps until the flashes were no longer detected. Fixation stability and the PRL for static fixation were also measured monocularly, using a 10-second fixation target. The foveal pit was located using the radial scan function of the OCT. If the foveal pit in one eye was difficult to locate because of disease progression, we based our estimate on the foveal pit location in the participant's other eye (Rohrschneider, 2004). We did this for participants M1 and B6.

Estimating the union of the scotomata in the two eyes

We calculated the region of stereo loss as the union of the scotoma maps in the two eyes (i.e., any retinal region with stereo loss in either eye would lead to a loss of stereopsis). To determine corresponding retinal locations in the two eyes, we assumed that our participants' eyes were aligned during binocular viewing, as most individuals with MD appear to align their gaze with the PRL in the dominant eye when viewing binocularly (Kabanarou, Crossland, Bellmann, Rees, Culham, & Rubin, 2006; Tarita-Nistor, Brent, Steinbach, & González, 2012). This assumption allowed us to superimpose the retinal maps of the two eyes, aligned on the foveae to estimate locations capable of mediating stereopsis (see Figure 2 in Verghese & Ghahghaei, 2020). We used the software created by Ghahghaei and Walker (2016) to obtain monocular graded vision loss maps from microperimetry and then

used a threshold to calculate the scotoma boundaries. (The various steps for the measurement of fixation stability, microperimetry, estimation of graded vision loss maps, and thresholding these maps are illustrated in Figure 2 of Verghese & Ghahghaei, 2020.) We then used the location of the foveal pit estimated from the

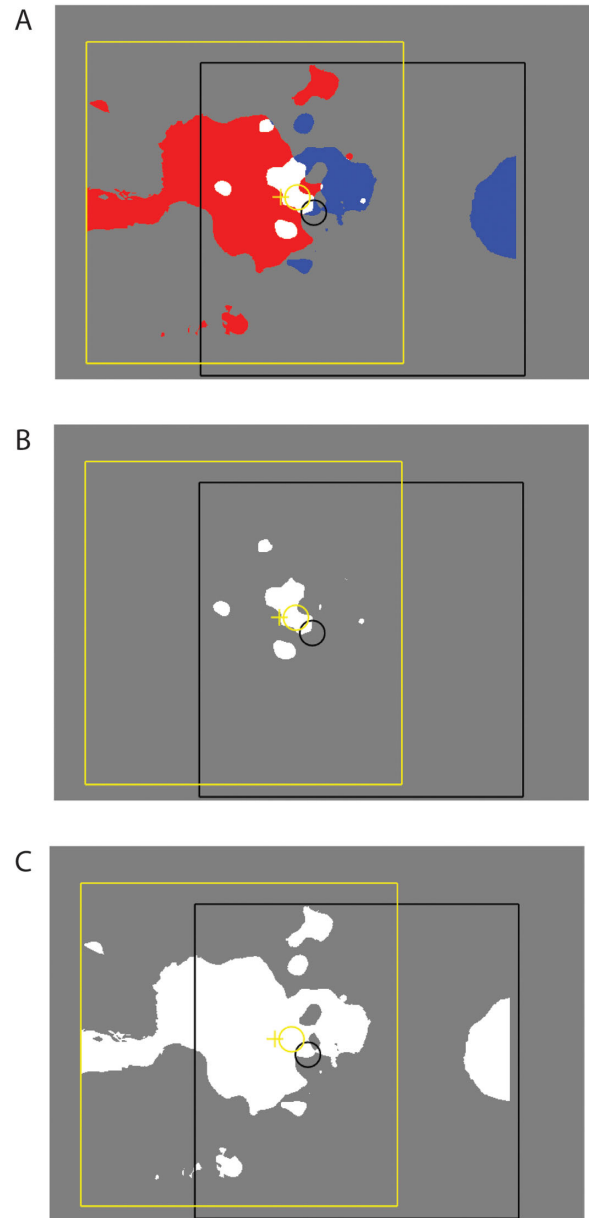


Figure 2. (A) Superimposed scotoma maps from the left eye (red) and right eye (blue) aligned on the fovea (yellow cross) for participant B3. The region of overlap of the scotomata of the two eyes is shown in white. The black and yellow circles represent the location of the left- and right-eye PRLs. (B) The binocular scotoma is the region of overlap, or the intersection of the scotomata in the two eyes. (C) The predicted stereoblind zone included the union of the scotomata in the two eyes or regions having vision loss in either eye.

OCT to align the scotoma maps from the two eyes as described previously (Verghese et al., 2016; Verghese & Ghahghaei, 2020). Figure 2A plots the scotoma maps from the two eyes aligned on the fovea (yellow cross). The left and right eye maps are shown in red and blue, respectively, with the region of overlap representing the binocular scotoma shown in white. Thus, the binocular scotoma corresponds to the intersection of the maps from the two eyes (replotted in Figure 2B). However, the region of stereo loss corresponds to the region with vision loss in *either* eye, or the union of the scotomata in the two eyes (Figure 2C).

Threshold analysis of scotoma

To generate the boundaries of participants' scotomata, we modified the Ghahghaei and Walker (2016) method, which used a threshold value for the smoothed scotoma maps that best approximated the microperimetry by eye, to instead find the threshold value that was the best quantitative fit to the seen and missed microperimetry points in the smoothed vision loss maps produced by the graphical user interface. The smoothed functional vision maps ranged from 0 to 1, with 0 indicating likely scotoma and 1 indicating intact vision. Scotoma/non-scotoma region predictions were generated for each participant with thresholds ranging from 0.1 to 0.9, in steps of 0.1. To calculate the extent of the scotoma, we varied the threshold and calculated the best-fitting scotoma/non-scotoma regions that captured missed/seen microperimetry points, respectively. To measure goodness of fit, the generated scotoma region was characterized by d' ; the proportion of hits corresponded to the missed flash locations that fell within the scotoma, and the proportion of false alarms corresponded to the seen flash locations that (incorrectly) fell inside the scotoma. We chose the threshold that yielded the highest d' to parse participants' graded vision loss maps into discrete non-scotoma regions.

Note that, when calculating the goodness-of-fit d' , we weighted the hit and false-alarm rates to account for large differences in the underlying count of points; generally, there were many more seen than missed microperimetry points. To weight the proportions, we multiplied hit and false-alarm rates by the proportion of the microperimetry data seen or missed, respectively.

Alignment of stereoperimetry maps and prediction from monocular scotomata

The alignment of participants' scotoma maps was compared with their performance in the stereoperimetry

experiment. We used an in/out alignment procedure to determine which target locations (using the center coordinates of the target) fell inside a participant's predicted union scotoma. An alignment score was calculated for all target locations using the participants' sensitivity to depth. Aligned locations were those stereo targets with center coordinates inside a participant's scotoma and $d' < 1$ or with center coordinates outside a participant's scotoma and $d' \geq 1$. Misaligned locations were those inside the scotoma with $d' \geq 1$ or those outside the scotoma with $d' < 1$.

Results

Stereoperimetry

We first measured stereoperimetry in four control participants at the fovea and at eccentricities of 1°, 2.5°, 5°, and 10°. The tested locations were displayed with respect to the fovea at the origin. Figure 3A plots d' at each of the tested locations using a color scale that displays perfect performance as bright green and complete stereoblindness as black. The data show that the large 20-arcmin step was detected across the visual field. For participant C3 we included targets at 15° eccentricity, as well, but did not test the upper visual field. The only locations where this participant lacked stereopsis were two locations at 15° along the horizontal meridian, left and right of the fovea, which coincided with the distance of the blind spots from the fovea as measured in the OCT/SLO, demonstrating that stereopsis is impacted when either eye lacks functional vision at a corresponding retinal location.

Next, we measured stereoperimetry for our MD participants. Figure 3B plots the stereoperimetry maps for individuals with a monocular scotoma (M1, M2, and M3) and an individual with non-overlapping scotomata in the two eyes (M4). Importantly, all of these participants had intact binocular fields. It is clear that each of these participants had a loss of stereopsis in the central field, despite intact binocular fields. Figure 3C plots stereoperimetry maps for our seven participants with overlapping scotomata in both eyes (B1–B7), resulting in a binocular scotoma and central field loss. These participants also had a loss of stereopsis in their central fields. For those with more extensive binocular scotomata in their upper visual field (B4, B5, and B6), we focused on residual stereopsis in the lower visual field. Figure 3C shows that coarse stereopsis is preserved in the periphery, despite the loss of stereopsis in the central visual fields. For participant B6, we used a disparity step of 30 arcmins because the standard 20-arcmin step was not visible. B6 had a binocular PRL at an eccentricity of 16° and a central scotoma that was at least 30° in diameter.

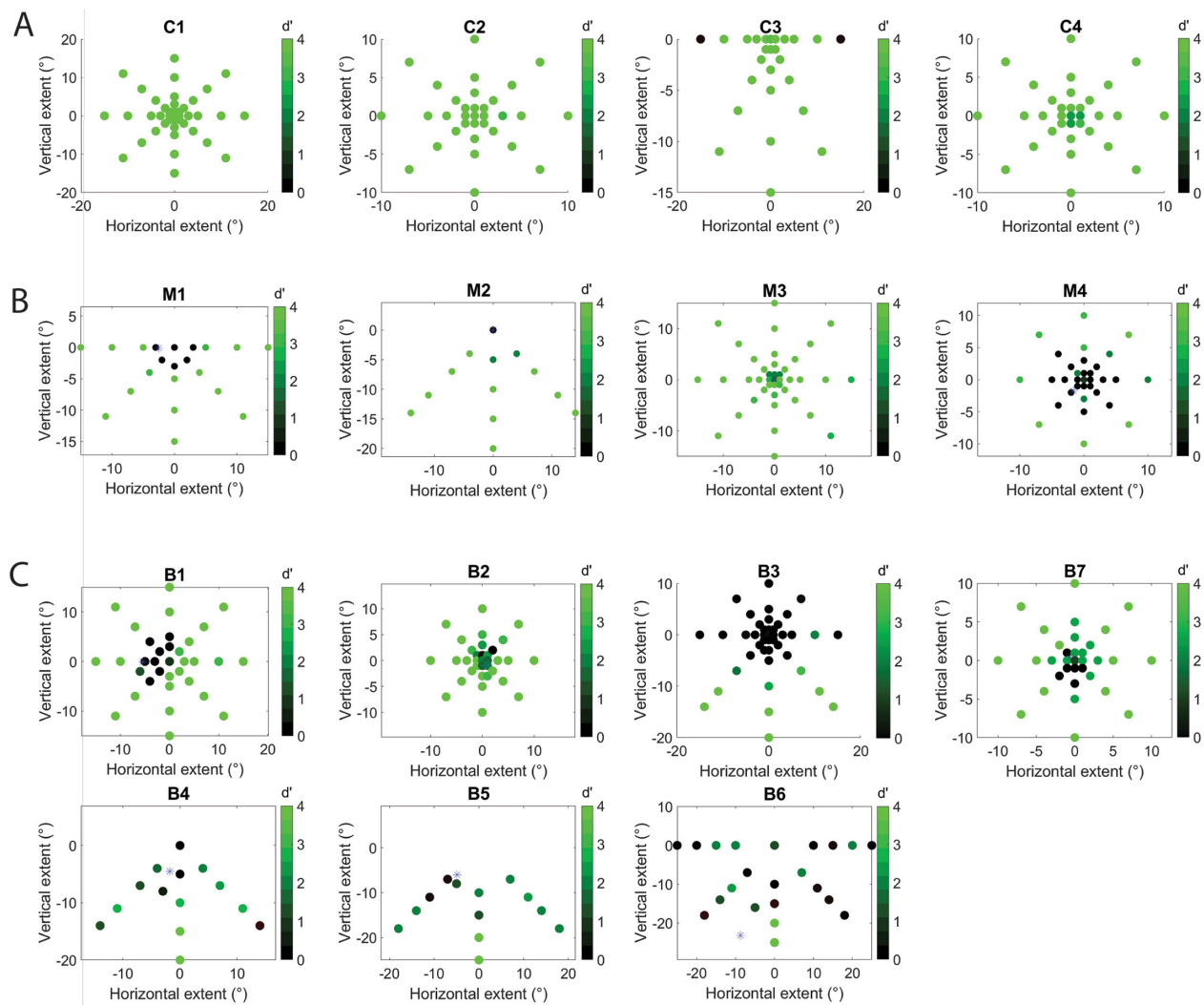


Figure 3. Stereoperimetry maps for controls (A), individuals with monocular or non-overlapping scotomata and no central field loss (B), and individuals with overlapping binocular scotomata and central field loss (C). Each panel plots the detectability (d') of a stereoscopically defined target at a particular location in the visual field with respect to the fovea (coordinates [0, 0]). The color bar represents d' values ranging between inability to detect the depth target (black) to perfect detection (bright green). The asterisks in each panel in (C) indicate the location of the PRL in the dominant eye.

Comparison of stereoperimetry with predicted regions of stereo loss

For each participant with macular degeneration, we compared the pattern of stereo loss measured by stereoperimetry to the predicted pattern from the union of the scotoma maps from the two eyes. Figure 4A shows the comparison for the monocular scotoma group that included individuals' monocular scotomata (M1, M2, and M3) or non-overlapping scotomata in the two eyes (M4). The predicted scotoma regions (shown in pink) correspond to the monocular scotoma for participants M1, M2, and M3 and to the union of the scotomata of two eyes for M4. For purposes of comparison, these maps are overlaid on the stereoperimetry data from Figure 3. A perfect prediction would show impaired stereopsis in the

pink regions and normal stereopsis outside these regions (see B1 and B3 in Figure 4B). Overall, the alignment between the stereoperimetry data and the predictions is good, but not perfect. Although there is good agreement between the presence of stereopsis and the scotoma-free regions, the composite scotoma map aligned less well with the stereoblind regions for some participants (M1 and M4). For M1, we suspect that that the misalignment was because we did not have a good estimate of the foveal pit location due to the poor quality of the retinal topography images. For M4 (and M2), we think that mapping the absolute scotoma might have underestimated the region of visual impairment in the two eyes. We return to these potential causes for misalignment between the stereoperimetry and the predicted maps in the Discussion.

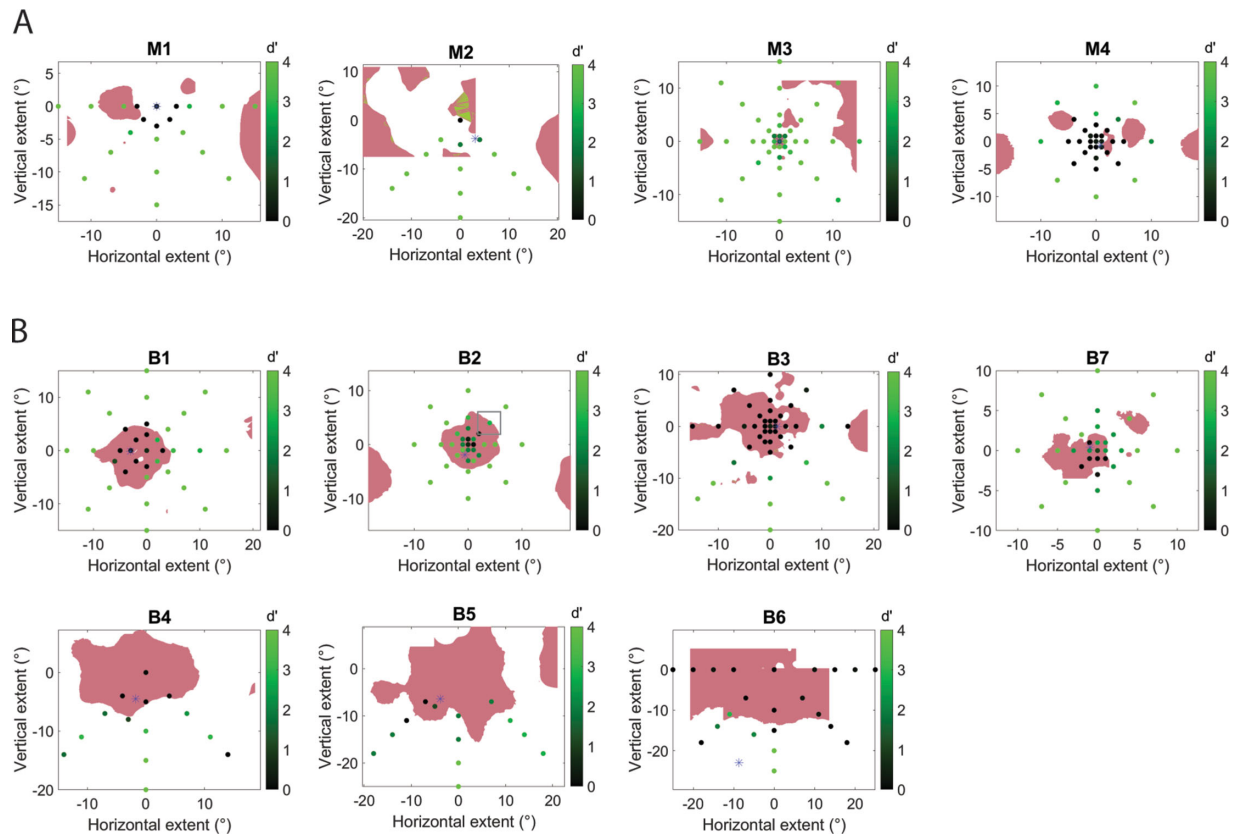


Figure 4. Comparison of the predicted zones of stereo loss from the union of the scotoma maps in the two eyes to the stereoperimetry data from Figures 3B and 3C. (A) Comparison for the monocular scotoma group that includes individuals with a scotoma in only one eye (M1, M2, and M3) and an individual with non-overlapping scotomata in the two eyes (M4). (B) Comparison for the binocular scotoma group. The square outline demonstrates that the target could have spanned regions inside and outside the scotoma.

Figure 4B compares stereoperimetry data and the predicted regions of stereo loss for individuals in the binocular scotoma group, who had central field loss due to overlapping scotomata in the two eyes. These individuals had an eccentric PRL as shown by the asterisk in each panel. In general, participants in the binocular scotoma group had more extensive scotomata and therefore more extensive regions of stereo loss than the monocular scotoma group. This is because the stereoblind regions included regions with a binocular scotoma (vision loss in overlapping regions of both eyes) and regions with monocular vision loss (or non-overlapping vision loss in the two eyes). As for the alignment between measurement and prediction, we can see good overlap between regions with poor stereo sensitivity ($d' < 1$) and predicted regions of stereo loss (pink) for observers with less extensive scotomata (B1, B2, B3, and B7). However, a small number of locations that showed good stereopsis were located within the predicted union scotoma region near the boundary (bright green points in pink regions). We attribute this to part of the target falling outside the predicted stereoblind zone (the outline of the target is represented by a gray outline in Figure 4B). Recall that we m -scaled the target

size with eccentricity according to the function $1 + (\text{eccentricity}/3)$, so that the $1^\circ \times 1^\circ$ target square in the fovea increased to a 2° square at an eccentricity of 3° , to a 3° square at an eccentricity of 6° , and so on. Thus, the plotted stereoperimetry locations (the center of the square target region) increasingly underestimate the extent of the target at larger eccentricities. Thus, even though their centers were located within the scotoma, part of the target could have fallen on corresponding locations with intact retina in both eyes.

For participants B3 and B7, we were able to measure the relative scotoma in the two eyes by using flashes of variable contrast during the microperimetry and measuring the contrast threshold at which the flashes were detected. To compare these to our other plots, we chose a threshold of 8 dB (corresponding to a Weber fraction of 2 in the Optos SLO) and labeled locations that required higher contrast as being within the scotoma. It is clear that varying the contrast of the points and including points with elevated contrast thresholds as part of the scotoma yielded good agreement between the predicted scotoma maps and the measured stereoperimetry (Figure 4B; see also Figure 5).

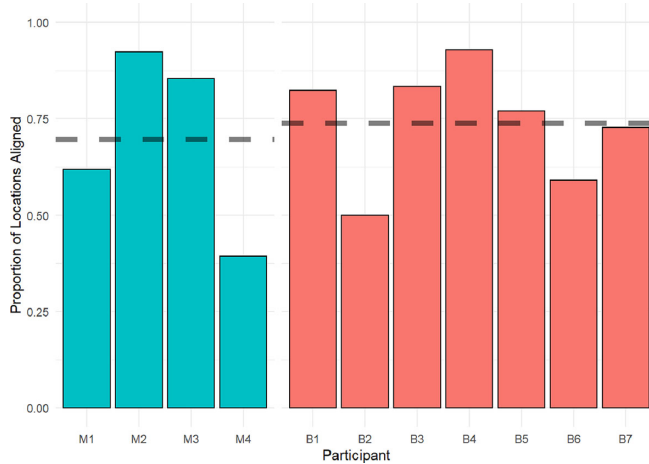


Figure 5. Alignment of the stereoperimetry measurement and the prediction from the scotoma maps. The proportion of the stereoperimetry points that are aligned with the union of the scotomata of the two eyes is plotted for each individual participant. Blue and pink bars represent individuals in the monocular and binocular scotoma groups, respectively. The dashed horizontal lines represent the mean alignment for the two groups.

The second row of Figure 4B shows the comparison between stereoperimetry and the prediction for individuals with large scotomata in the two eyes. Here, we see poor stereopsis within the predicted stereoblind zone and intact stereopsis in the far periphery, despite the large extent of the scotomata. However, there are also locations where the stereoperimetry and union prediction do not align: A closer inspection indicates impaired stereopsis outside the predicted stereoblind zone. There are several potential explanations for this discrepancy. First, the prediction was based on measurement of the absolute scotoma, which can underestimate the region of visual impairment. Second, the scan angle in the SLO did not allow us to map the entire extent of the scotoma. This is particularly evident for B6 (the straight edges indicate limits imposed by the scan angle of the SLO, rather than the true extent of the scotoma).

Overall, the alignment between the measured stereoperimetry and the predicted union of the monocular scotomata is quite good. Figure 5 shows the alignment score for each of our macular degeneration participants, as outlined in the Methods. Briefly, aligned locations are stereo targets with center coordinates inside a participant's scotoma and $d' < 1$ or with center coordinates outside a participant's scotoma and $d' \geq 1$. Misaligned locations are those inside the scotoma with $d' \geq 1$ or those outside the scotoma with $d' < 1$. The pink and blue bars plot the data for individuals in the binocular and monocular scotoma groups, respectively. Although there is variability in the alignment scores across individual participants, the average alignment score (horizontal dashed line) for participants in the

monocular scotoma group is 72% and for participants in the binocular scotoma group it is 75%. Recall that the alignment score includes poor stereo within the scotoma boundary and good stereo outside the boundary.

We calculated whether this alignment could have occurred by chance—whether the probability of a location having impaired/intact stereopsis was independent of whether it was within/outside the union scotoma. If the fraction of points with poor stereopsis ($d' < 1$) relative to the total number of stereo locations tested is a and the fraction of points within the predicted union is b , then the probability that two random draws, one from the stereoperimetry data and one from the scotoma data, would result in a point with poor stereopsis and a point within the scotoma is ab . Similarly, the probability that the random draws would pick one point with good stereopsis and one point outside the scotoma is $(1 - a)(1 - b)$. The sum of these two quantities represents the probability that the stereoperimetry data will align with the scotoma data by chance.

We calculated the predicted alignment by chance and compared it to the actual alignment between stereoperimetry and the union scotoma for each individual. For individuals in the binocular scotoma group ($n = 7$), the measured alignment was significantly better than chance (Wilcoxon matched-pairs signed-rank test, $P < 0.02$). For those in the monocular scotoma group ($n = 4$), the measured alignment was not significantly better than chance (Wilcoxon matched-pairs signed-rank test, $P = 0.99$), likely because the n is small and because the proportion of healthy retina and locations with peripheral stereopsis are both large, which results in the term $(1 - a)(1 - b)$ being much larger than the term ab .

Discussion

We measured local stereopsis across the visual field for controls, for individuals with non-overlapping scotomata and no field defect, and for individuals with overlapping scotomata and a field defect. Our results show that, for individuals with macular degeneration, coarse stereopsis is preserved in the periphery and that stereopsis is impacted in regions broadly consistent with missing retinal input in either eye.

We compared our measurement of local stereopsis to the prediction of the union of the scotomata in the two eyes (i.e., that stereopsis would be impacted in a region with vision loss in either eye). A point-by-point comparison between locations of stereo loss/intact stereo and the predictions from the superposition of the scotomata of each eye is good, averaging 72% alignment for those with a monocular scotoma and 75% for those with a binocular scotoma. Thus, our results are generally consistent with the union prediction

and show that individuals with MD with a scotoma in only one eye or non-overlapping scotomata in the two eyes have stereoblind regions despite intact visual fields. Individuals with field loss due to overlapping scotomata in the two eyes have more extensive regions of stereoblindness surrounding the binocular scotoma. Importantly, both groups of individuals have coarse stereopsis outside the affected region, in peripheral retina.

Limitations

Although we have general agreement between measures of local stereopsis and the prediction from the union scotoma, several factors potentially impacted the alignment between measurement and prediction. One of the limitations of this study is that eye position was not monitored because of the challenges of monitoring eye position remotely with the EyeLink desktop configuration in conjunction with the stereo shutter glasses, particularly for participants with eccentric gaze. Observers were asked to fixate the PRL marker, and we typically displayed targets at the marker at least four times more frequently than at other locations, encouraging observers to maintain fixation. However, the display duration of 3 seconds potentially allowed ample time for eye movements. Even so, the alignment of the stereoperimetry is impressive.

Previous studies have indicated that, during binocular viewing, gaze is typically aligned with the PRL of the dominant eye (Kabanarou et al., 2006; Tarita-Nistor et al., 2012), even when the two eyes have PRLs at different locations relative to the fovea. Although we assumed that the gaze of the two eyes is aligned, we cannot be sure if observers were fixating on the plane of the screen, as we did not monitor fixation. To determine how the relative position of the scotoma of the two eyes would change if the observer fixated at a different depth than the fixation screen, we considered fixation in front of or behind the screen that resulted in offsets between the location of the foveae of the two eyes (and their respective scotomata). For fixation distances that resulted in crossed and uncrossed offsets of up to 4° between the eyes, we did not see an overall improvement in the alignment between the stereoperimetry and the union of the scotoma maps (see Supplementary Figure S1). For most participants, this range of offsets did not change alignment significantly; for one participant (M1), the alignment improved by about 25% when considering fixation in a plane about 10 cm in front of the display screen.

Another factor that could explain some of the discrepancies between stereoperimetry and the prediction from the scotomata of the two eyes is that the alignment of the stereoperimetry and the union scotoma was based on the *center* of the stereo target

falling within the boundary of the union scotoma and did not take the extent of the target into account. Because the target size scaled with eccentricity, it is possible that a part of the target whose center was located just within the border of a monocular/binocular scotoma fell on intact retinal regions just outside the scotoma and was detected. This could have led to stereoperimetry measurements indicating intact stereopsis within the boundary of the union scotoma as in the case of participant B2. Thus, the extent of the target falling on both intact and stereoblind retina could have been a factor that affected alignment between stereoperimetry and prediction, particularly at more eccentric locations where the target size increased with eccentricity according to $1 + (\text{eccentricity}/3)$ (e.g., the target subtended $3^\circ \times 3^\circ$ and $6^\circ \times 6^\circ$ at eccentricities of 6° and 15° , respectively). Supplementary Figure S2 plots the fraction of the target that was visible at each tested location.

Finally, another potential source of misalignment could arise from our measurement of the absolute monocular scotoma in maculopathy observers rather than the relative scotoma. Estimating scotoma boundaries based on the absolute scotoma potentially ignores differences in contrast sensitivity at corresponding locations due to a relative scotoma. Previous studies indicate that differences in the contrast of the half images in the two eyes impair stereoacuity (Legge & Gu, 1989; Smallman & McKee, 1995). Thus, the difference in perceived contrast due to differences in scotoma density at corresponding locations could potentially have impaired stereopsis, although it is not clear that it would have affected the detection of the large disparity step that we used. The ideal approach would have been to measure the relative scotoma by reducing the contrast of the flash in 2-dB steps until the flash was no longer visible. However, MD participants typically fatigue with the increased time required to map selected locations in 2-dB contrast steps, resulting in worsening fixation stability and the SLO pausing because it cannot visualize the selected region of interest. Thus, measuring the relative scotoma for all observers, although desirable, was not realistic, especially for individuals with extended scotomata and poor fixation stability. It is worth noting that the two individuals for whom we were able to map the relative scotoma showed the best alignment with their stereoperimetry data.

Implications of monocular/binocular central scotomata in real life

The central retina in one eye may be affected well before the other, especially at the onset of wet macular degeneration. While this may leave the binocular visual field and good acuity intact, the loss of central vision in

one eye impacts stereopsis. Individuals tend to use the high-acuity central retina in the unaffected eye, ignoring the potential for stereopsis in the periphery. This is true for individuals with monocular/non-overlapping scotomata such as M2 and M4, as well as for those with asymmetric scotomata such as B1 and B3. For example, these individuals did not have measurable stereoacuity according to the Randot Stereo Test (worse than 30 arcmins in [Table 1](#)), but our stereoperimetry measurements indicated that they were able to detect coarse disparity steps of 20 arcmins in their periphery. Thus, the periphery clearly has the ability to detect disparity.

Of course, individuals with scotomata in both eyes are also stereoblind in a part of the visual field that has vision loss in either eye. When individuals with binocular scotomata have similar patterns of vision loss in the two eyes, they appear better able to use their peripheral stereopsis, perhaps because the PRLs in the two eyes are in roughly similar locations and are closer to regions with intact retina in both eyes ([Verghese & Ghahghaei, 2020](#)). Although there is evidence that individuals switch PRLs depending on the light level ([Lei & Schuchard, 1997](#)), during reading ([Déruaz, Whatham, Mermoud, & Safran, 2002](#)), and during pursuit ([Shanidze, Fusco, Potapchuk, Heinen, & Verghese, 2015](#)), it is not clear whether individuals with PRLs in different locations in the two eyes switch PRLs from the dominant-eye PRL to a peripheral locus with intact retina in both eyes when they switch from a task that benefits from acuity to one that benefits from stereopsis.

A relevant question is whether the periphery of individuals with macular degeneration has the stereoacuity necessary for tasks of everyday living. As stereoacuity declines with eccentricity ([Fendick & Westheimer, 1983](#); [McKee, Welch, Taylor, & Bowne, 1990](#)), the residual stereoacuity in maculopathy depends on the eccentricity of healthy retina in corresponding locations in the two eyes. Recall that, whereas binocular acuity is determined by the less impacted eye, stereoacuity requires intact retina loci in both eyes and is thus determined by the eye with the greater extent of vision loss. An inspection of [Table 1](#) shows that maculopathy participants in our study had PRLs in their non-dominant eye (typically the eye with the larger scotoma) ranging from eccentricities of 1° to over 17°. Larger scotomata are associated with dry macular degeneration, such that the affected retina can extend beyond the macula (which typically extends to about 8° eccentricity) ([Hood, 2015](#)). The smaller scotoma diameters are associated with wet macular degeneration treated with anti-vascular endothelial growth factor injection therapy that typically limit the scotoma diameter to 10°, or an eccentricity of 5°. To determine how stereoacuity falls off with eccentricities up to 15°, we measured stereoacuity in the lower

visual field using side-by-side rectangular patches of random dots that scaled with eccentricity ([Ghahghaei, McKee & Verghese, 2016](#)). The goal was to estimate the lower-bound (best) stereoacuity that the participants with MD could achieve at various eccentricities in the periphery, depending on the size of their scotoma. For control participants, stereoacuity thresholds were less than 0.5 arcmins at an eccentricity of 6°, consistent with other studies where the disparity stimuli were scaled with eccentricity ([Fendick & Westheimer, 1983](#); [McKee et al., 1990](#)), about 1 minute of arc at an eccentricity of 9°, and less than 3 minutes of arc at an eccentricity of 15°. So, in theory, PRLs at eccentricities of 5° to 9° have stereoacuity thresholds around 1 arcmin, which is adequate for many eye–hand coordination tasks such as picking up a cup by its handle or placing pegs in a peg board ([Verghese et al., 2016](#)). Even a PRL at an eccentricity of 15° is capable of detecting a curb drop-off of about 15 cm, which has a disparity of 3 to 10 arcmins depending on the distance from the curb (2–0.7 m for an individual with eyes at a height of 1.65 m and an interocular separation of 6.5°). Thus, the intact periphery in maculopathy could indeed support the coarse stereoacuity required for eye–hand coordination and mobility.

Utility of stereoperimetry

All our participants, including those who failed clinical tests of stereopsis (see [Table 1](#)), had regions in the periphery supporting coarse stereopsis. Individuals with asymmetric scotomata in the two eyes likely performed poorly on the Randot Stereo Test because they fixated the small stereo target with their better-eye PRL, which did not necessarily correspond to an intact retinal location in the other eye. At the same time, our results show that peripheral stimuli scaled with eccentricity revealed the presence of coarse stereopsis in all participants. This observation suggests two things: First, the Randot Stereo Test is an inadequate measure of the potential of peripheral stereopsis (see also [Chopin, Chan, Guellai, Bavelier, & Levi, 2019](#)), and, second, a more careful estimate of stereo threshold with stimuli scaled to the eccentricity of the non-dominant eye PRL is necessary to determine the presence of potentially useful stereopsis in the periphery. Importantly, our participants had coarse stereopsis in the lower visual field, which is beneficial for eye–hand coordination ([Melmoth et al., 2009](#); [Cao & Markowitz, 2014](#); [Verghese et al., 2016](#)), for walking ([Bonnen et al., 2019](#); [Buckley et al., 2010](#); [Hayhoe et al., 2009](#)), for negotiating steps and curbs, and for decreasing the risk of falls ([Lord & Mayhew, 2001](#)). By revealing the presence of coarse stereopsis in the periphery and by providing a method to map it, our study provides information about loci that

can potentially be trained for these tasks of daily living.

Keywords: macular degeneration, peripheral stereopsis, stereoperimetry

Acknowledgments

The authors thank Suzanne McKee and Natela Shnidze for their comments on the manuscript. Some of these results were presented at the annual meeting of the Vision Sciences Society in 2021.

Supported by a grant from the National Eye Institute, National Institutes of Health (R01 EY027390 to PV).

Commercial relationships: none.

Corresponding author: Preeti Verghese.

Email: preeti@ski.org.

Address: Smith-Kettlewell Eye Research Institute, San Francisco, CA, USA.

References

- Bonnen, K., Matthis, J. A., Gibaldi, A., Banks, M. S., Levi, D. M., & Hayhoe, M. (2019). A role for stereopsis in walking over complex terrains. *Journal of Vision*, *19*(10), 178b, <https://doi.org/10.1167/19.10.178b>.
- Brainard, D. H. (1997). The Psychophysics Toolbox. *Spatial Vision*, *10*(4), 433–436.
- Buckley, J. G., Panesar, G. K., MacLellan, M. J., Pacey, I. E., & Barrett, B. T. (2010). Changes to control of adaptive gait in individuals with long-standing reduced stereoacuity. *Investigative Ophthalmology & Visual Science*, *51*(5), 2487.
- Cao, K. Y., & Markowitz, S. N. (2014). Residual stereopsis in age-related macular degeneration and its impact on vision-related abilities: A pilot study. *Journal of Optometry*, *7*(2), 100–105.
- Chopin, A., Chan, S. W., Guellai, B., Bavelier, D., & Levi, D. M. (2019). Binocular and non-stereoscopic cues can deceive clinical tests of stereopsis. *Sci. Rep.*, *9*(1), 5789.
- Cheung, S., & Legge, G. E. (2005). Functional and cortical adaptations to central vision loss. *Visual Neuroscience*, *22*(2), 187–201.
- Chung, S. T. L. (2011). Improving reading speed for people with central vision loss through perceptual learning. *Investigative Ophthalmology & Visual Science*, *52*(2), 1164–1170.
- Déruaz, A., Whatham, A. R., Mermoud, C., & Safran, A. B. (2002). Reading with multiple preferred retinal loci: Implications for training a more efficient reading strategy. *Vision Research*, *42*(27), 2947–2957.
- Fendick, M., & Westheimer, G. (1983). Effects of practice and the separation of test targets on foveal and peripheral stereoacuity. *Vision Research*, *23*(2), 145–150.
- Fine, E. M., & Peli, E. (1995). Scrolled and rapid serial visual presentation texts are read at similar rates by the visually impaired. *Journal of the Optical Society of America A: Optics, Image Sciences, and Vision*, *12*(10), 2286–2292.
- Fletcher, D. C., Schuchard, R. A., & Watson, G. (1999). Relative locations of macular scotomas near the PRL: Effect on low vision reading. *Journal of Rehabilitation Research and Development*, *35*(4), 356–364.
- Ghahghaei, S., McKee, S., & Verghese, P. (2016). The precision of stereopsis in the lower visual field. *Journal of Vision*, *16*(12), 826–826, <https://doi.org/10.1167/16.12.826>.
- Ghahghaei, S., McKee, S. P., & Verghese, P. (2019). The upper disparity limit increases gradually with eccentricity. *Journal of Vision*, *19*(11):3, 1–12, <https://doi.org/10.1167/19.11.3>.
- Ghahghaei, S., & Walker, L. (2016). SKERI-Optos: A graphical user interface to map scotoma and PRL with the Optos OCT/SLO. *Journal of Vision*, *16*(4), 40–41, <https://doi.org/10.1167/16.4.41>.
- Hayhoe, M., Gillam, B., Chajka, K., & Vecellio, E. (2009). The role of binocular vision in walking. *Visual Neuroscience*, *26*(1), 73.
- Hood, D. C. (2015). Imaging glaucoma. *Annual Review of Vision Science*, *1*, 51–72.
- Hubschman, J. P., Reddy, S., & Schwartz, S. D. (2009). Age-related macular degeneration: Current treatments. *Clinical Ophthalmology*, *3*, 155–166.
- Kabanarou, S. A., Crossland, M. D., Bellmann, C., Rees, A., Culham, L. E., & Rubin, G S. (2006). Gaze changes with binocular versus monocular viewing in age-related macular degeneration. *Ophthalmology*, *113*(12), 2251–2258.
- Klein, R., Chou, C. F., Klein, B. E., Zhang, X., Meuer, S. M., & Saaddine, J. B. (2011). Prevalence of age-related macular degeneration in the US populations. *Archives of Ophthalmology*, *129*(1), 75–80.
- Lei, H., & Schuchard, R. A. (1997). Using two preferred retinal loci for different lighting conditions in patients with central scotomas. *Investigative Ophthalmology & Visual Science*, *38*(9), 1812–1818.

- Legge, G. E., Ross, J. A., Isenberg, L. M., & LaMay, J. M. (1992). Psychophysics of reading. Clinical predictors of low-vision reading speed. *Investigative Ophthalmology and Visual Science*, 33(3), 677–687.
- Legge, G. E., & Gu, Y. C. (1989). Stereopsis and contrast. *Vision Research*, 29(8), 989–1004.
- Lord, S. R., & Mayhew, J. (2001). Visual risk factors for falls in older people. *Journal of the American Geriatrics Society*, 49(5), 508–515.
- McKee, S. P., Welch, L., Taylor, D. G., & Bowne, S. F. (1990). Finding the common bond: Stereoacuity and the other hyperacuties. *Vision Research*, 30(6), 879–891.
- Melmoth, D. R., Finlay, A. L., Morgan, M. J., & Grant, S. (2009). Grasping deficits and adaptations in adults with stereo vision losses. *Investigative Ophthalmology & Visual Science*, 50(8), 3711–3720.
- Niechwiej-Szwedo, E., Colpa, L., & Wong, A. M. F. (2019). Visuomotor behaviour in amblyopia: Deficits and compensatory adaptations. *Neural Plasticity*, 2019, 6817839.
- Pelli, D. G. (1997). The VideoToolbox software for visual psychophysics: Transforming numbers into movies. *Spatial Vision*, 10(4), 437–442.
- Rohrschneider, K. (2004). Determination of the location of the fovea on the fundus. *Investigative Ophthalmology & Visual Science*, 45(9), 3257–3258.
- Rovamo, J., & Virsu, V. (1979). An estimation and application of the human cortical magnification factor. *Experimental Brain Research*, 37(3), 495–510.
- Schuchard, R. A., Naseer, S., & de Castro, K. (1999). Characteristics of AMD patients with low vision receiving visual rehabilitation. *Journal of Rehabilitation Research and Development*, 36(4), 294–302.
- Shanidze, N., Fusco, G., Potapchuk, E., Heinen, S. J., & Verghese, P. (2015). Smooth pursuit eye movements in patients with macular degeneration. *Journal of Vision*, 16(3):1, 1–14, <https://doi.org/10.1167/16.3.1>.
- Shanidze, N., Heinen, S., & Verghese, P. (2017). Monocular and binocular smooth pursuit in central field loss. *Vision Research*, 141, 181–190.
- Smallman, H. S., & McKee, S. P. (1995). A contrast ratio constraint on stereo matching. *Proceedings of the Royal Society B: Biological Sciences*, 260(1359), 265–271.
- Tarita-Nistor, L., Brent, M. H., Steinbach, M. J., & González, E. G. (2012). Fixation patterns in maculopathy: From binocular to monocular viewing. *Optometry and Vision Science*, 89(3), 277–287.
- Verghese, P., Tyson, T. L., Ghahghaei, S., & Fletcher, D. C. (2016). Depth perception and grasp in central field loss. *Investigative Ophthalmology & Visual Science*, 57(3), 1476–1487.
- Verghese, P., & Ghahghaei, S. (2018). Stereo perimetry reveals peripheral loci mediating coarse stereopsis in macular degeneration. *Journal of Vision*, 18(10), 996, <https://doi.org/10.1167/18.10.996>.
- Verghese, P., & Ghahghaei, S. (2020). Predicting stereopsis in macular degeneration. *Journal of Neuroscience*, 40(28), 5465–5470.
- Vullings, C., & Verghese, P. (2021). Mapping the binocular scotoma in macular degeneration. *Journal of Vision*, 21(3):9, 1–12, <https://doi.org/10.1167/jov.21.3.9>.
- Wardle, S. G., Bex, P. J., Cass, J., & Alais, D. (2012). Stereoacuity in the periphery is limited by internal noise. *Journal of Vision*, 12(6):12, 1–12, <https://doi.org/10.1167/12.6.12>.
- White, J. M., & Bedell, H. E. (1990). The oculomotor reference in humans with bilateral macular disease. *Investigative Ophthalmology & Visual Science*, 31(6), 1149–1161.